NATIONAL ADVISORY COMMITTEE FOR AERONAUTICS

TECHNICAL NOTE

No. 1714

PLATE COMPRESSIVE STRENGTH OF FS-1h MAGNESIUM-ALLOY SHEET AND A MAXIMUM-STRENGTH FORMULA FOR MAGNESIUM-ALLOY AND ALUMINUM-ALLOY FORMED SECTIONS

By George L. Gallaher

Langley Aeronautical Laboratory
Langley Field, Va.

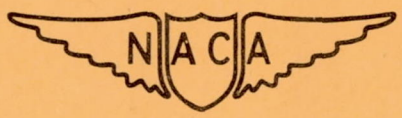

Washington
October 1948

NATIONAL ADVISORY COMMITTEE FOR AERONAUTICS

TECHNICAL NOTE NO. 1714

PLATE COMPRESSIVE STRENGTH OF FS-1h MAGNESIUM-ALLOY SHEET AND A MAXIMUM-STRENGTH FORMULA FOR MAGNESIUM-ALLOY AND ALUMINUM-ALLOY FORMED SECTIONS

By George L. Gallaher

SUMMARY

The plate compressive strength of FS-1h magnesium-alloy sheet was determined from local-instability tests of formed Z-section columns. The critical compressive stress was found to correlate well with the compressive stress-strain curve for the material. The curves of average stress at maximum load plotted against calculated elastic critical strain resulted in a family of curves similar to previous results for aluminum-alloy sheet.

An empirical formula was developed for calculating the average stress at maximum load for formed Z-sections and channel sections of FS-1h magnesium-alloy sheet and 24S-T and 17S-T aluminum-alloy sheet.

INTRODUCTION

Recent investigations by the National Advisory Committee for Aeronautics have provided information on the plate compressive strength of various aluminum and magnesium alloys. From these investigations, the buckling stress and average stress at maximum load have been quite well-established for extruded aluminum and magnesium alloys. (See reference 1.) For sheet materials, however, the plate compressive strength has not been so generally established. The only information available was obtained from tests of formed Z-sections and channel sections of 17S-T and 24S-T aluminum-alloy sheet (references 2 and 3, respectively) and no data are available for magnesium-alloy sheet. Inasmuch as the test results for the aluminum-alloy sheet materials were essentially different from those obtained for the extruded materials, particularly with regard to the average stress at maximum load, additional information on the plate compressive strength of sheet materials is required.

Because data on magnesium sheet were not available, experimental data were obtained on the plate compressive strength of FS-1h magnesium-alloy sheet. Results are presented for the buckling stress and the average

stress at maximum load for FS-1h magnesium-alloy formed Z-sections. The results for the average stress at maximum load are also analyzed and compared with those obtained for aluminum-alloy sheet (references 2 and 3).

SYMBOLS

A	cross-sectional area of specimen
b_D	developed width of plate (A/t)
b_F	width of flange of Z-section
b_W	width of web of Z-section
C	empirical constant used in maximum-load formula
E	Young's modulus of elasticity in compression, taken as 6500 ksi for FS-1h magnesium alloy
k_W	nondimensional coefficient used in plate-buckling formula
L	length of column
P_{max}	maximum load
t	thickness of plate
ϵ_{cr}	calculated elastic critical compressive strain
μ	Poisson's ratio, taken as 0.3 for FS-1h magnesium alloy
σ_{cr}	critical compressive stress
σ_{cy}	compressive yield stress
$\bar{\sigma}_{max}$	average compressive stress at maximum load

METHODS OF TESTING AND ANALYSIS

All tests were made in hydraulic testing machines accurate to within three-fourths of 1 percent. The ends of the stress-strain specimens and the formed Z-sections were ground flat and square. The Z-section specimens were all cut from two 4- by 12-foot sheets of 0.102-gage FS-1h magnesium alloy and were hot formed. The specimens were fabricated by the manufacturer, and the forming operations were reported to be that the

forming was done at temperatures under 320° F and the time at maximum temperature prior to making each bend was limited to 10 minutes. Dies were heated by hand torch and were probably in the range of 200° to 280° F. Hot forming is generally required for bending magnesium sheet because it has hexagonal crystals with only one slip plane. In the forming process, the material was bent across the grain; thus, the grain direction of the material was parallel to the longitudinal axis of the Z-section test specimens.

Stress-strain curves.- The compressive stress-strain curves for the flat sheet (obtained only for the with-grain direction) were made autographically by tests of single-thickness specimens in a modified Montgomery-Templin type of compression fixture. The correct support for the flat magnesium compression specimens was difficult to obtain. Lueder's lines developed and the magnesium tended to slip and wedge between the supports. Similar difficulties were encountered in the investigation reported in reference 4.

For the formed material in the corners, compression specimens were cut from the corner portion and tested in a special compression fixture. This fixture provided continuous support along the length of the specimen of the type illustrated in figure 1. A wire strain gage was placed on the inside of the corner and the load-strain curve was recorded autographically.

Plate compressive strength.- The plate compressive strength of the material was obtained from compression tests of formed Z-section columns so proportioned as to develop local instability; that is, instability of the plate elements of which the columns are comprised. The lengths of the columns were chosen so that three half-waves would be obtained when buckling occurred. (See reference 5.) The columns were tested with the flat ends bearing directly against the testing-machine heads. In these local-instability tests, measurements were taken of the cross-sectional distortion, and the critical stress was taken as the stress corresponding to the critical load at the top of the knee of the load-distortion curve, as illustrated in figure 2. The method of measuring the cross-sectional distortion by use of a variable-differential-transformer-type gage is shown in figure 3. (A variable-differential-transformer-type gage consists of a coil with three windings and an iron core. The coil windings are such that the induced voltage is a sensitive measure of the core position.) The measuring apparatus is essentially a parallel-rule linkwork mechanism with the upper rule held stationary on a conventional dial-gage stand. The gage coil is attached to this stationary upper rule. The lower rule is free to swing laterally and holds the core of the gage and a straightedge. The straightedge rests against a flange of the specimen and picks up the buckles wherever they develop. This method proved quite successful and permitted a minute force from the buckles to register distortion on the measuring apparatus.

RESULTS AND DISCUSSION

Compressive Properties

The compressive properties of the two original flat 4- by 12-foot FS-1h magnesium-alloy sheets used for making the test specimens were essentially the same. In fact, the compressive yield stresses had a range of less than 1 ksi for all the flat specimens and less than 2 ksi for the curved specimens. The modulus of elasticity in compression was taken as 6500 ksi for magnesium alloy.

The average compressive stress-strain curves for specimens cut from the original material before forming, from the flat portions of the flanges and webs after forming, and from the formed material in the corners are shown in figure 4. Inspection of these curves reveals that hot forming of the Z-section test specimens did not appreciably change the compressive stress-strain curve of the flat portions of the flanges and webs, whereas in the formed corners the compressive yield stress was raised about 13 percent.

Plate Compressive Strength

The results of the local-instability tests of the formed Z-section columns, used to determine the plate compressive strength, are given in table 1.

For purposes of comparison with a compressive stress-strain curve, the test data are plotted against the calculated elastic critical compressive strain ϵ_{cr}. The formula for ϵ_{cr} is the plate buckling formula for the elastic critical compressive stress divided by E:

$$\epsilon_{cr} = k_w \frac{\pi^2}{12(1 - \mu^2)} \left(\frac{t}{b_w}\right)^2 \qquad (1)$$

The method of dimensioning and the value of k_w may be obtained from figure 5; the data for k_w were obtained from reference 6. Figure 6 shows the critical stress σ_{cr} and the average stress at maximum load σ_{max} plotted against ϵ_{cr}. The two stress-strain curves shown represent the upper- and the lower-limit curves found for the FS-1h sheet material in the flanges and webs of the formed Z-sections.

The buckling data appear to follow the lower-limit stress-strain curve quite well. Because of this agreement, the reduced modulus of

elasticity for plate buckling may be approximated by the secant modulus. (The use of the secant modulus has previously been suggested in references 1 and 7.) The critical compressive stress may therefore be evaluated for practical purposes as the product of ϵ_{cr} and the secant modulus or directly from the compressive stress-strain curve for the material, given the calculated value of ϵ_{cr}. The results obtained by the foregoing method tend to be somewhat unconservative in most cases unless a lower-limit compressive stress-strain curve is used. This result agrees with the theory in reference 8 for plastic buckling of plates.

The test data in figure 6 show that the secant modulus may also be used to predict the maximum strength in some instances because σ_{cr} and $\bar{\sigma}_{max}$ occur quite close together at high stresses. When $\bar{\sigma}_{max}$ occurs at lower stresses, figure 7 may be more useful in estimating $\bar{\sigma}_{max}$. In figure 7 the data are identified according to b_w/t ratios. Such a plot of $\bar{\sigma}_{max}$ against ϵ_{cr} results in a family of curves dependent upon the ratio b_w/t. Similar results have been found for 17S-T and 24S-T aluminum-alloy sheet (references 2 and 3). In order to illustrate the difference between $\bar{\sigma}_{max}$ and σ_{cr} the variation of σ_{cr} with $\sigma_{cr}/\bar{\sigma}_{max}$ is shown in figure 8.

Empirical Maximum-Strength Formula

A study of local-instability test data for extruded aluminum and magnesium Z-sections (reference 1) shows that the $\bar{\sigma}_{max}$ data apparently plot against ϵ_{cr} as a single curve. References 2 and 3, however, as well as the present paper, show that formed Z-sections develop a family of $\bar{\sigma}_{max}$ curves for different b_w/t ratios. The separate $\bar{\sigma}_{max}$ curves were believed to occur because the corners of sections formed from sheet material have higher compressive properties than the rest of the section. Since a Z-section (or a channel section) with a large value of b_w/t has a smaller percentage of this high-strength corner area than one with a small value of b_w/t, the family of curves appeared to be a reasonable result. Investigation of the FS-1h data, however, showed that the percentage of high-strength corner area accounted for only part of the spread in $\bar{\sigma}_{max}$. The investigation did reveal, however, that a reasonably straight-line relationship existed between $\bar{\sigma}_{max}$ and the percentage of corner area. Because the high-strength corner area was considered a constant for these data, this relationship has been plotted in figure 9 as $\bar{\sigma}_{max}$ against the reciprocal of the total area.

A study of the other available data (17S-T and 24S-T aluminum-alloy sheet in references 2 and 3, respectively) also showed a similar rela-

tionship between $\bar{\sigma}_{max}$ and total area. Figure 10 has been prepared to present an interesting feature found for the formed Z-sections of all three materials. Figure 10 is given for 24S-T aluminum-alloy formed Z-sections because the most complete and extensive data are available for them (reference 3). These Z-sections have approximately the same total area and the same value of $\bar{\sigma}_{max}$ but varying values of σ_{cr}. This result seems to indicate that, for formed Z-sections with identical corners, σ_{cr} depends upon the way in which the material is distributed between the web and flange while $\bar{\sigma}_{max}$ does not.

An attempt was made to correlate the test data for 24S-T and 17S-T aluminum alloy with the FS-1h magnesium-alloy test data as plotted in figure 9. The shape of the curved corners was slightly different (fig. 11) but the sections were considered to be near enough alike that this difference might be neglected. The different moduli, yield stresses, and thicknesses encountered made selection of parameters difficult. A formula somewhat similar to the maximum-load formula for a rectangular plate with simply supported edges

$$P_{max} = Ct^2 \sqrt{E\sigma_{cy}} \tag{2}$$

or

$$\frac{\bar{\sigma}_{max}}{\sqrt{E\sigma_{cy}}} = C \frac{t^2}{A} \tag{3}$$

found in reference 9 (p. 401) gave the best method of correlating the data. Plotting the nondimensional value of $\bar{\sigma}_{max}/\sqrt{E\sigma_{cy}}$ (where σ_{cy} is for the flat material in the specimen) against the nondimensional value of t^2/A proved quite effective. Figure 12 shows all the data for the formed Z-sections from this paper and from references 2 and 3 plotted in this manner. The cut-off line in figure 12 is necessary for the magnesium-alloy Z-sections and represents $\bar{\sigma}_{max}$ equal to σ_{cy}. Because the stress-strain curve for FS-1h magnesium alloy levels off at about the yield-stress value, $\bar{\sigma}_{max}$ cannot be expected to occur at stresses greater than σ_{cy}. For 17S-T and 24S-T aluminum alloys, however, the stress-strain curve continues to rise above the yield stress and, for the range of data available, no cut-off line appears necessary. The equation of the line through the combined data is

$$\frac{\bar{\sigma}_{max}}{\sqrt{E\sigma_{cy}}} = 2.14 \frac{t^2}{A} + 0.01 \tag{4}$$

The channel-section data of references 2 and 3 also fit along this line. The ratio t^2/A in equation (4) may also be written as t/b_D where b_D is the developed width equal to A/t.

It must be remembered that this formula is empirical and is derived only from the available data on formed Z-sections. Also, the data in this paper and references 2 and 3 are for Z-sections with b_F/b_W greater than 0.35 so that the flanges are primarily responsible for buckling (see fig. 5); for b_F/b_W less than this value, column failure rather than local instability is likely to occur for the lengths tested.

CONCLUSIONS

Curves for the plate compressive strength of FS-1h magnesium-alloy sheet have been established from tests on formed Z-sections.

An empirical formula is presented for the average stress at maximum load. The formula is nondimensional in form and gives strengths that agree closely with experimental results for FS-1h magnesium-alloy sheet, as well as for 17S-T and 24S-T aluminum-alloy sheet. Caution should be exercised in extending this formula to other materials.

Langley Aeronautical Laboratory
National Advisory Committee for Aeronautics
Langley Field, Va., July 20, 1948

REFERENCES

1. Heimerl, George J.: Determination of Plate Compressive Strengths. NACA TN No. 1480, 1947.

2. Heimerl, George J., and Roy, J. Albert: Column and Plate Compressive Strengths of Aircraft Structural Materials. 17S-T Aluminum-Alloy Sheet. NACA ARR No. L5F08, 1945.

3. Lundquist, Eugene E., Schuette, Evan H., Heimerl, George J., and Roy, J. Albert: Column and Plate Compressive Strengths of Aircraft Structural Materials. 24S-T Aluminum-Alloy Sheet. NACA ARR No. L5F01, 1945.

4. Moore, A. A., and McDonald, J. C.: Compression Testing of Magnesium Alloy Sheet. Proc. A.S.T.M., vol. 45, 1945, pp. 698-704.

5. Heimerl, George J., and Roy, J. Albert: Determination of Desirable Lengths of Z- and Channel-Section Columns for Local-Instability Tests. NACA RB No. L4H10, 1944.

6. Kroll, W. D., Fisher, Gordon P., and Heimerl, George J.: Charts for Calculation of the Critical Stress for Local Instability of Columns with I-, Z-, Channel-, and Rectangular-Tube Section. NACA ARR No. 3K04, 1943.

7. Gerard, George: Secant Modulus Method for Determining Plate Instability above the Proportional Limit. Jour. Aero. Sci., vol. 13, no. 1, Jan. 1946, pp. 38-44 and 48.

8. Stowell, Elbridge Z.: A Unified Theory of Plastic Buckling of Columns and Plates. NACA TN No. 1556, 1948.

9. Timoshenko, S.: Theory of Elastic Stability. McGraw-Hill Book Co., Inc., 1936, p. 401.

TABLE 1

DIMENSIONS AND TEST RESULTS FOR FS-1h MAGNESIUM-ALLOY FORMED Z-SECTION COLUMNS THAT DEVELOP LOCAL INSTABILITY

Column	t (in.)	b_W (in.)	b_F (in.)	L (in.)	A (sq in.)	$\frac{b_F}{b_W}$	$\frac{b_W}{t}$	k_W (from fig. 5)	ϵ_{cr} (a)	σ_{cr} (ksi)	$\bar{\sigma}_{max}$ (ksi)
1a	0.102	3.56	2.82	21.66	0.884	0.792	34.9	1.38	0.00102	6.1	13.9
1b	.101	3.55	2.84	21.67	.879	.800	35.1	1.35	.00099	6.7	13.8
1c	.101	3.55	2.82	21.66	.875	.795	35.1	1.37	.00101	5.4	14.3
2a	.103	3.57	2.51	20.30	.833	.704	34.7	1.68	.00127	8.6	14.9
2b	.102	3.56	2.51	20.30	.820	.705	34.9	1.68	.00125	7.8	14.8
2c	.102	3.55	2.50	20.30	.817	.705	34.8	1.68	.00126	7.8	15.1
3a	.102	3.59	2.02	18.47	.738	.563	35.2	2.43	.00179	11.9	15.8
3b	.102	3.56	2.02	18.48	.724	.568	34.9	2.39	.00177	11.9	15.7
3c	.101	3.53	2.02	18.48	.715	.572	35.0	2.36	.00174	11.5	15.8
4a	.102	3.53	1.70	17.13	.655	.481	34.6	3.06	.00231	15.3	17.3
4b	.102	3.52	1.70	17.13	.655	.482	34.5	3.06	.00232	15.0	17.1
4c	.102	3.53	1.70	17.12	.650	.481	34.6	3.06	.00231	14.8	16.9
5a	.101	2.90	2.28	17.48	.707	.786	28.7	1.40	.00154	9.3	16.5
5b	.101	2.94	2.27	17.47	.707	.773	29.1	1.44	.00154	9.9	16.2
5c	.100	2.91	2.28	17.48	.707	.784	29.1	1.41	.00151	10.7	16.2
6a	.101	2.91	2.00	16.15	.650	.687	28.8	1.75	.00191	12.9	17.5
6b	.101	2.93	1.99	16.16	.650	.680	29.0	1.78	.00192	13.2	17.2
6c	.101	2.96	1.99	16.15	.650	.672	29.3	1.82	.00192	12.3	17.1
7a	.102	2.88	1.63	14.93	.580	.565	28.2	2.41	.00274	18.8	19.3
7b	.102	2.91	1.61	14.94	.574	.553	28.5	2.50	.00278	17.8	19.0
7c	.101	2.91	1.60	14.94	.568	.550	28.8	2.52	.00273	18.3	19.3
8a	.101	2.87	1.35	13.71	.517	.470	28.4	3.15	.00354	22.0	22.4
8b	.101	2.91	1.34	13.70	.514	.460	28.8	3.22	.00351	21.1	21.7
8c	.101	2.92	1.32	13.71	.508	.451	28.9	3.28	.00356	21.7	22.3
9a	.104	2.24	1.57	12.83	.508	.701	21.5	1.68	.00328	21.7	22.3
9b	.102	2.25	1.57	12.83	.502	.698	22.0	1.69	.00316	19.5	21.1
9c	.102	2.25	1.56	12.83	.495	.692	22.0	1.70	.00317	20.6	21.3
10a	.103	2.28	1.29	11.25	.450	.565	22.1	2.41	.00446	25.3	25.6
10b	.102	2.29	1.29	11.24	.445	.562	22.4	2.43	.00440	24.9	25.1
10c	.101	2.28	1.28	11.23	.440	.561	22.6	2.44	.00434	24.8	25.5
11a	.102	2.24	1.07	9.06	.397	.478	22.0	3.08	.00577	25.7	26.4
11b	.101	2.22	1.07	9.06	.396	.482	22.0	3.06	.00572	25.2	26.2
11c	.102	2.20	1.08	9.06	.397	.491	21.6	2.98	.00579	25.3	25.8
12a	.102	1.80	1.21	7.75	.377	.672	17.6	1.81	.00529	24.9	25.6
12b	.102	1.79	1.20	7.74	.376	.670	17.5	1.82	.00539	25.5	26.5
12c	.102	1.79	1.20	7.74	.374	.670	17.5	1.82	.00539	25.1	26.2

NACA

[a] $\epsilon_{cr} = k_W \frac{\pi^2}{12(1-\mu^2)} \left(\frac{t}{b_W}\right)^2$

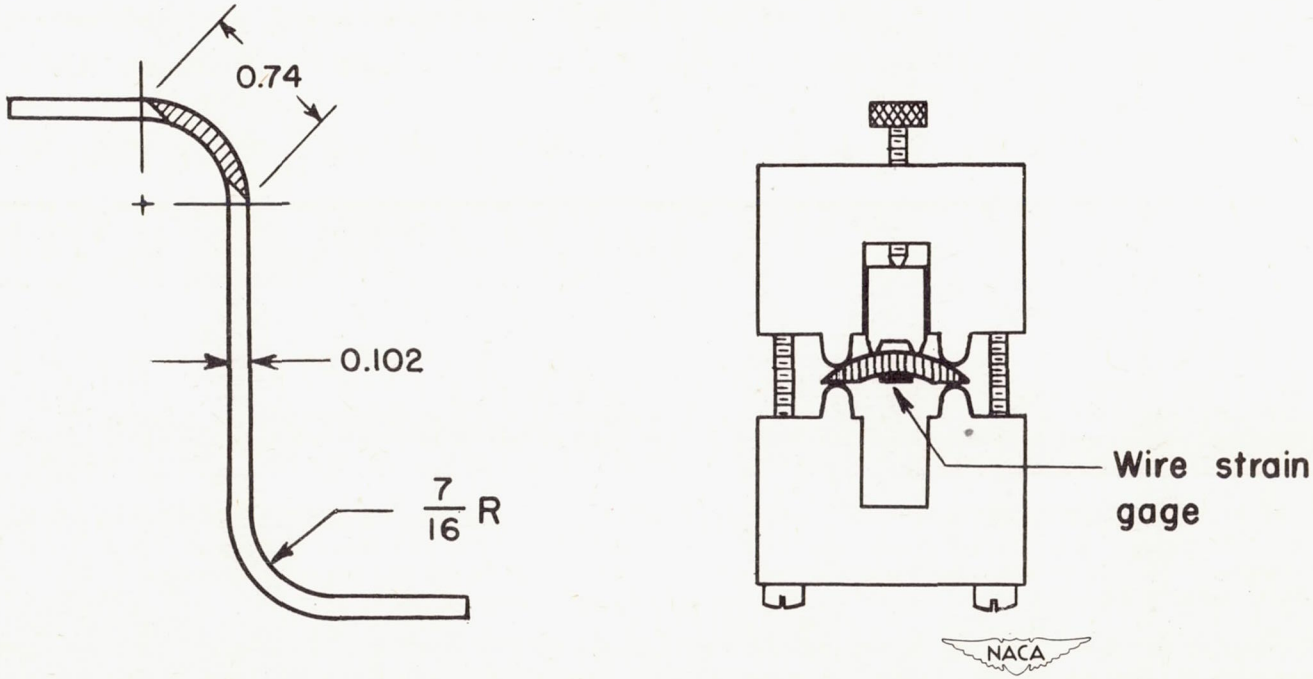

(a) Location.

(b) Supporting fixture.

Figure 1.— Curved compressive stress-strain specimen.

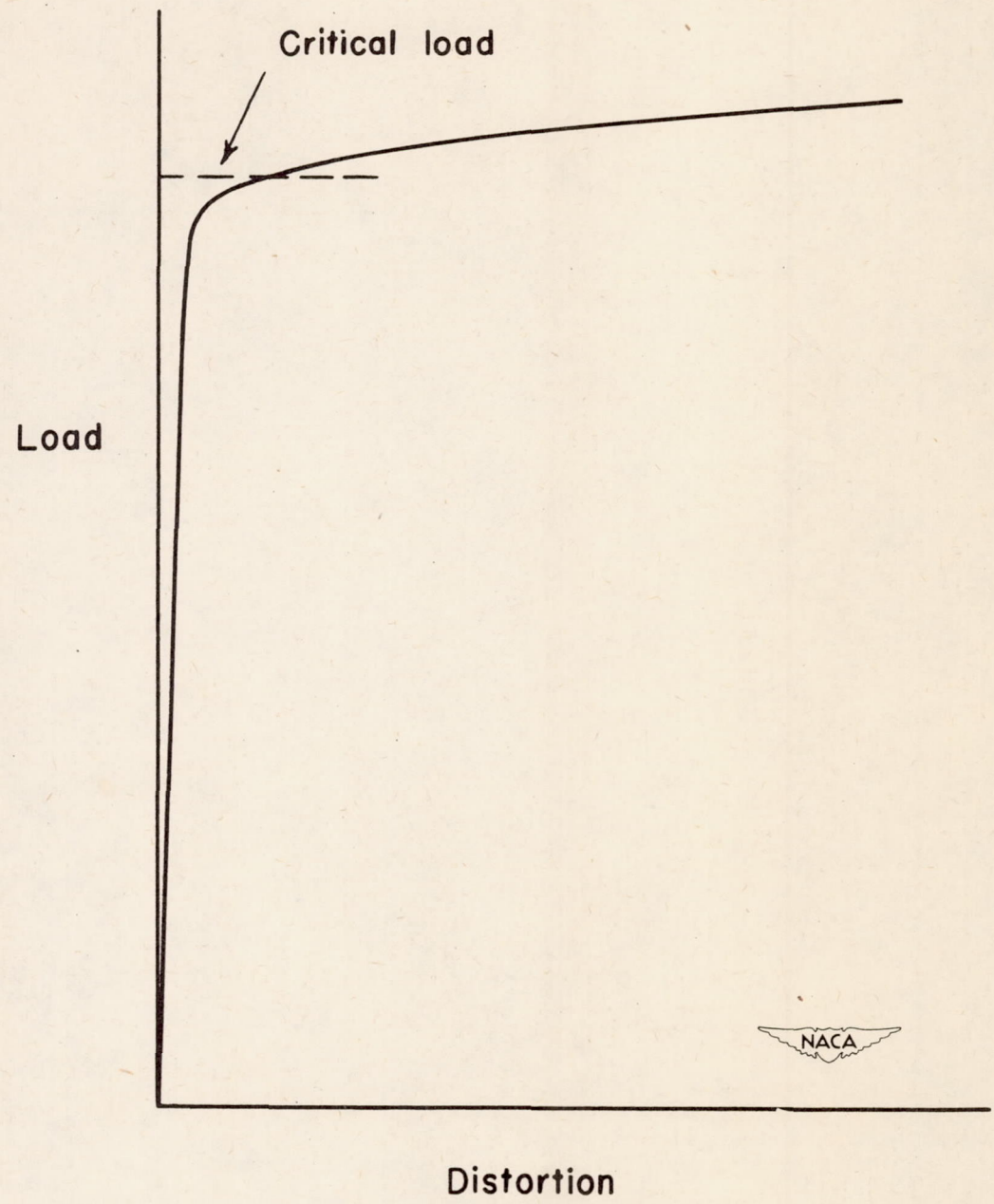

Figure 2.— Illustrative load-distortion curve.

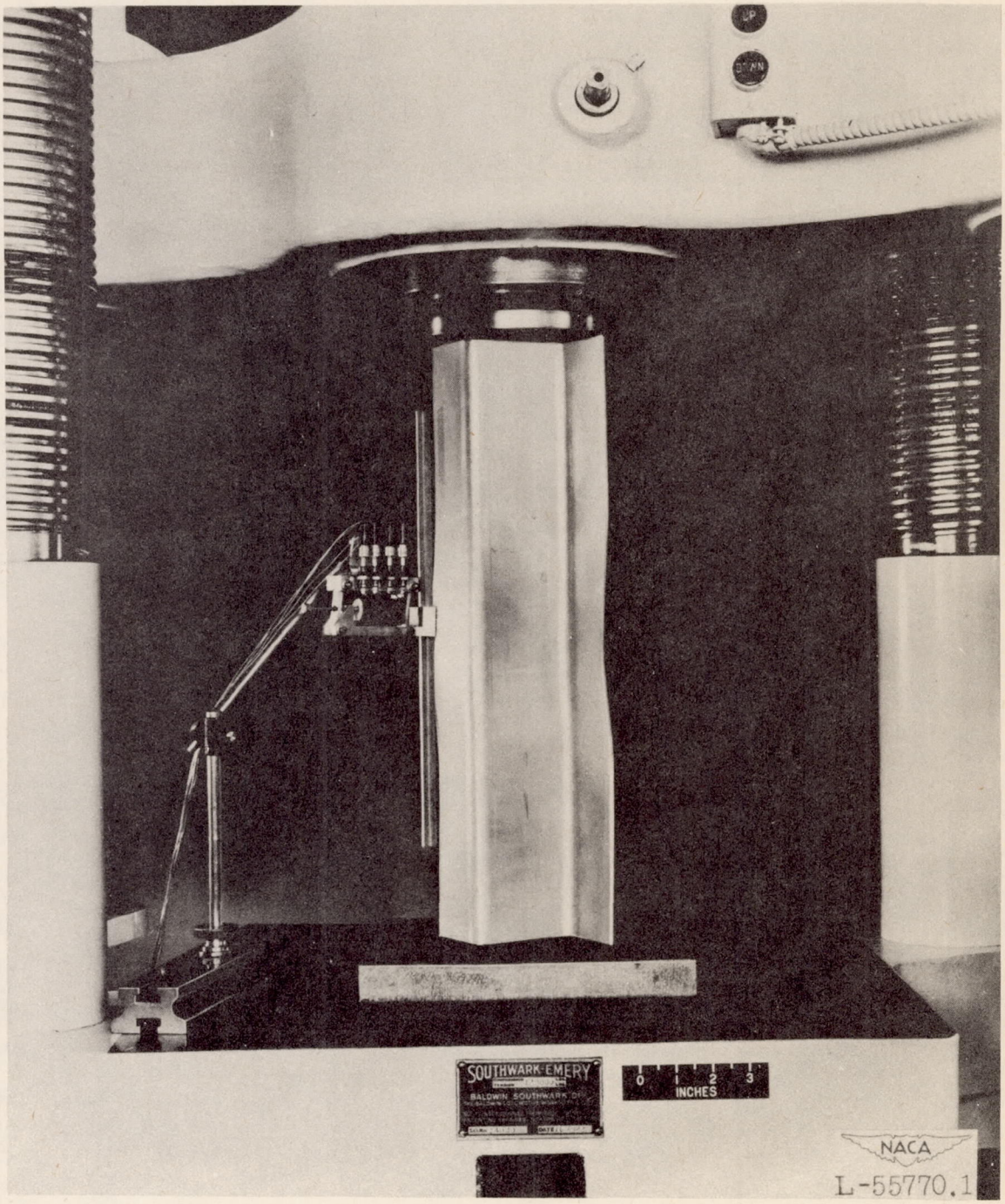

Figure 3.- Method of measuring cross-section distortion of a Z-section column.

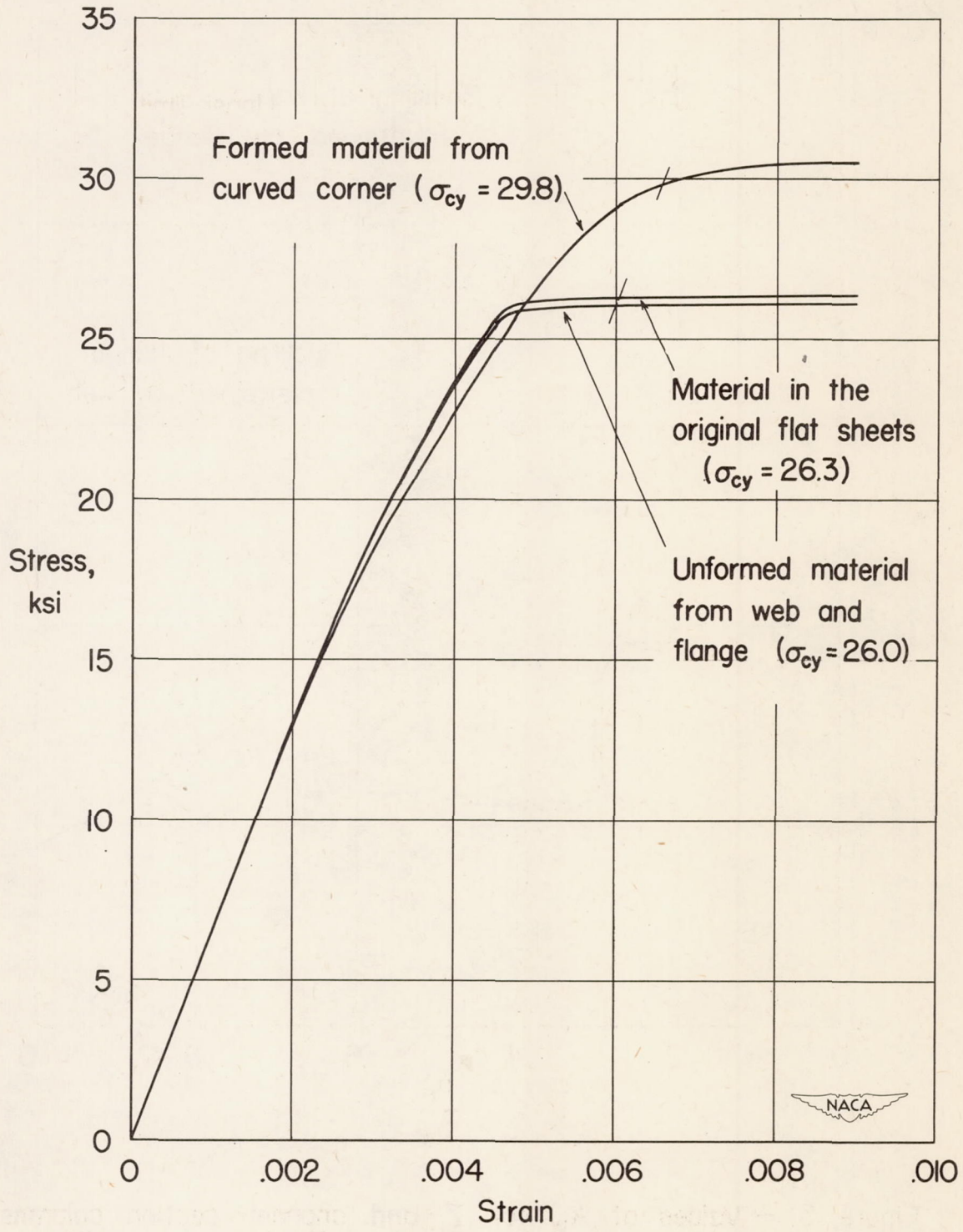

Figure 4.— Average compressive stress-strain curves for FS-1h magnesium-alloy sheet (with grain; t = 0.102 inch).

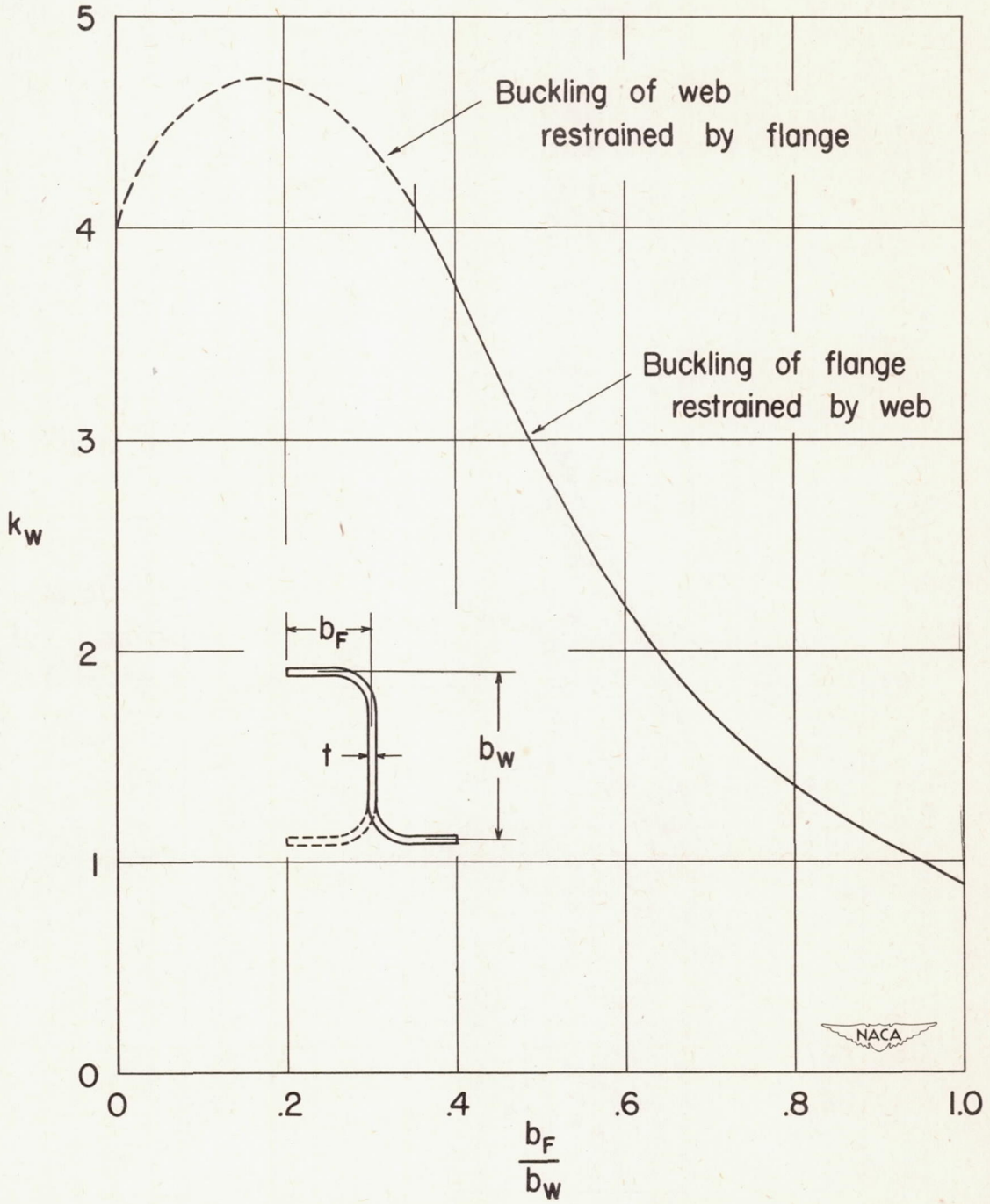

Figure 5. — Values of k_w for Z- and channel-section columns of uniform thickness (from reference 6).

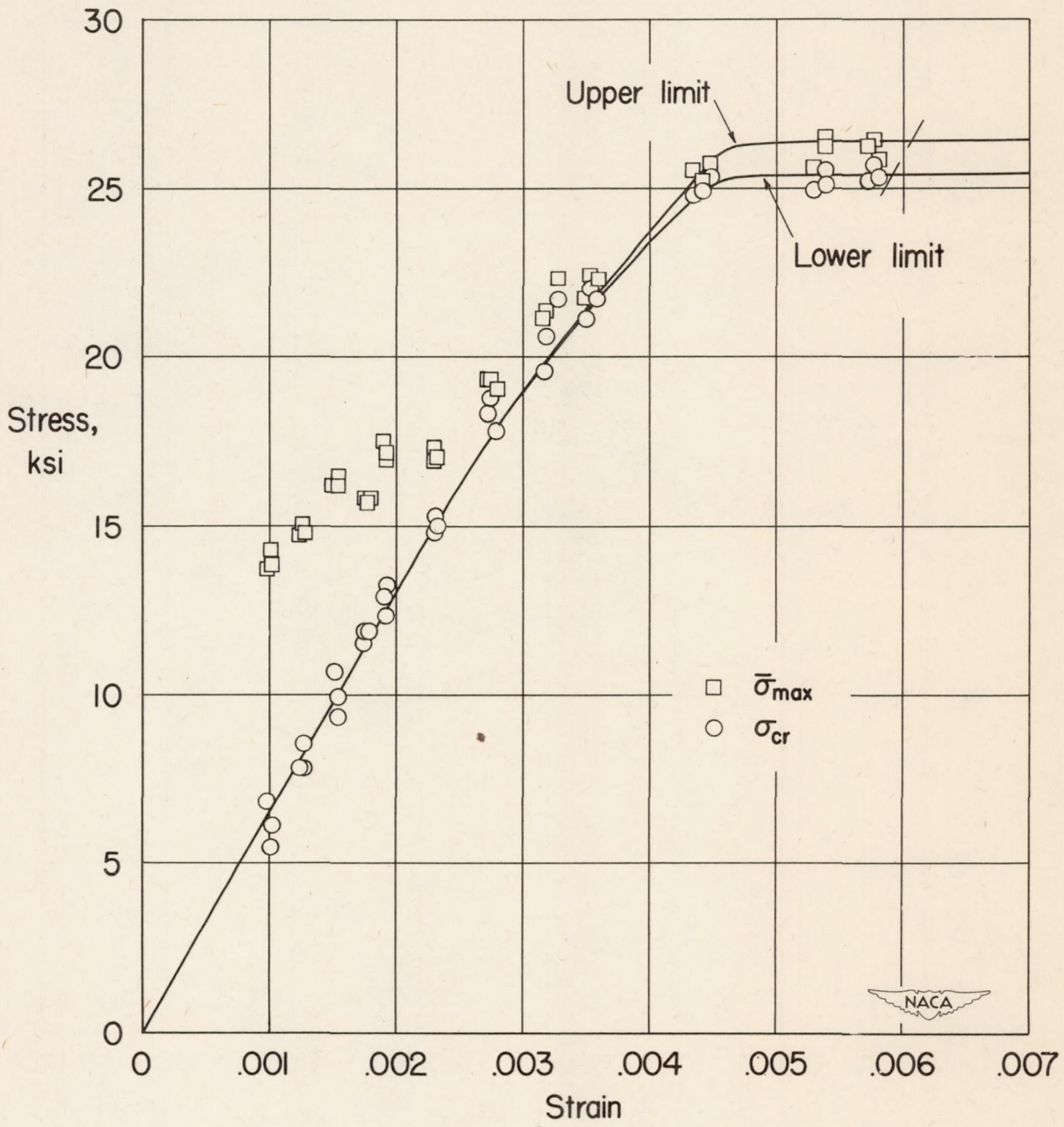

Figure 6.— Correlation of plate compressive test results with compressive stress-strain curves for FS-1h magnesium-alloy formed Z-sections. (Calculated elastic critical compressive strain used for plate tests.)

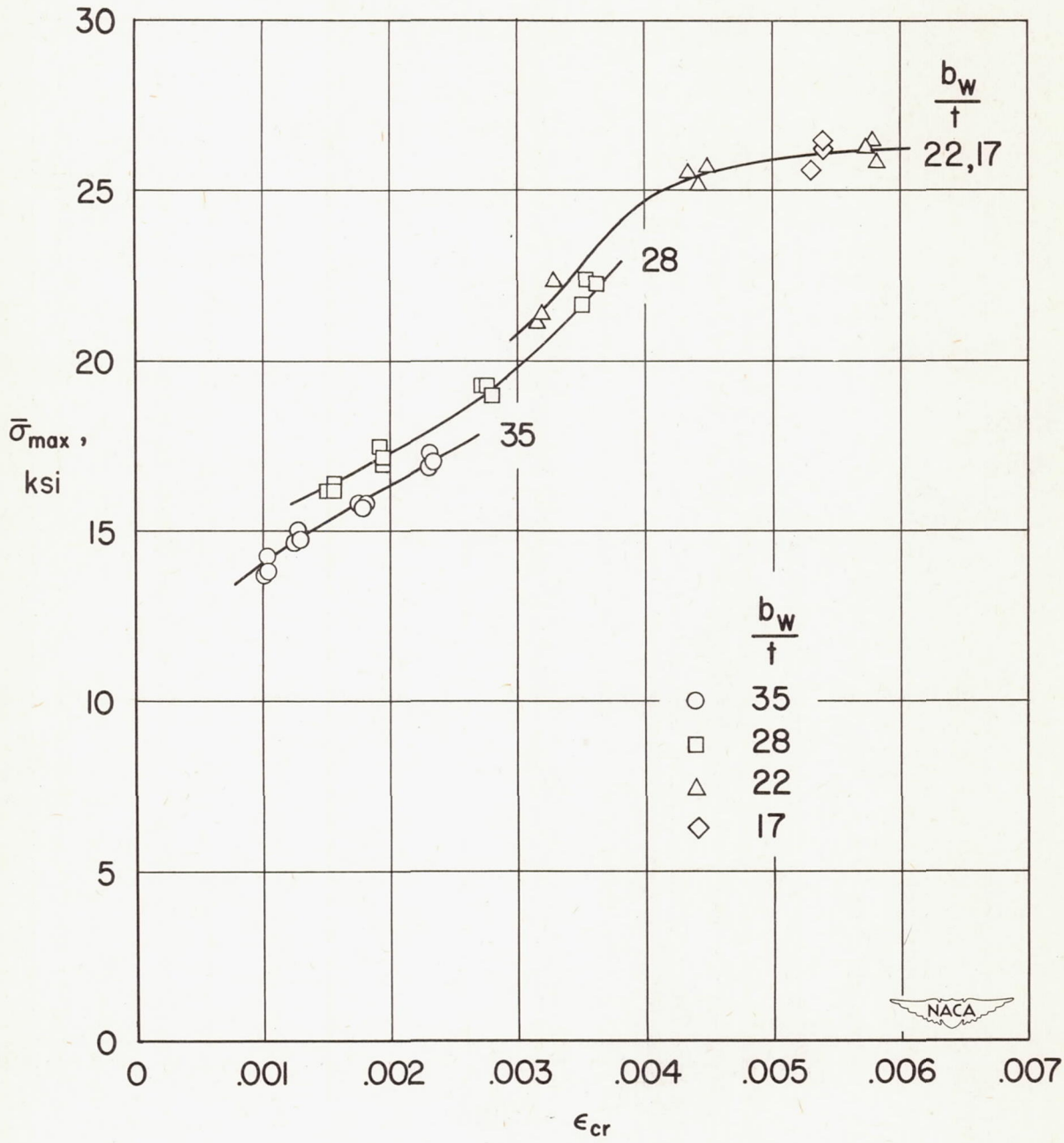

Figure 7. —Variation of $\bar{\sigma}_{max}$ with ϵ_{cr} for FS-1h magnesium-alloy formed Z-section columns.

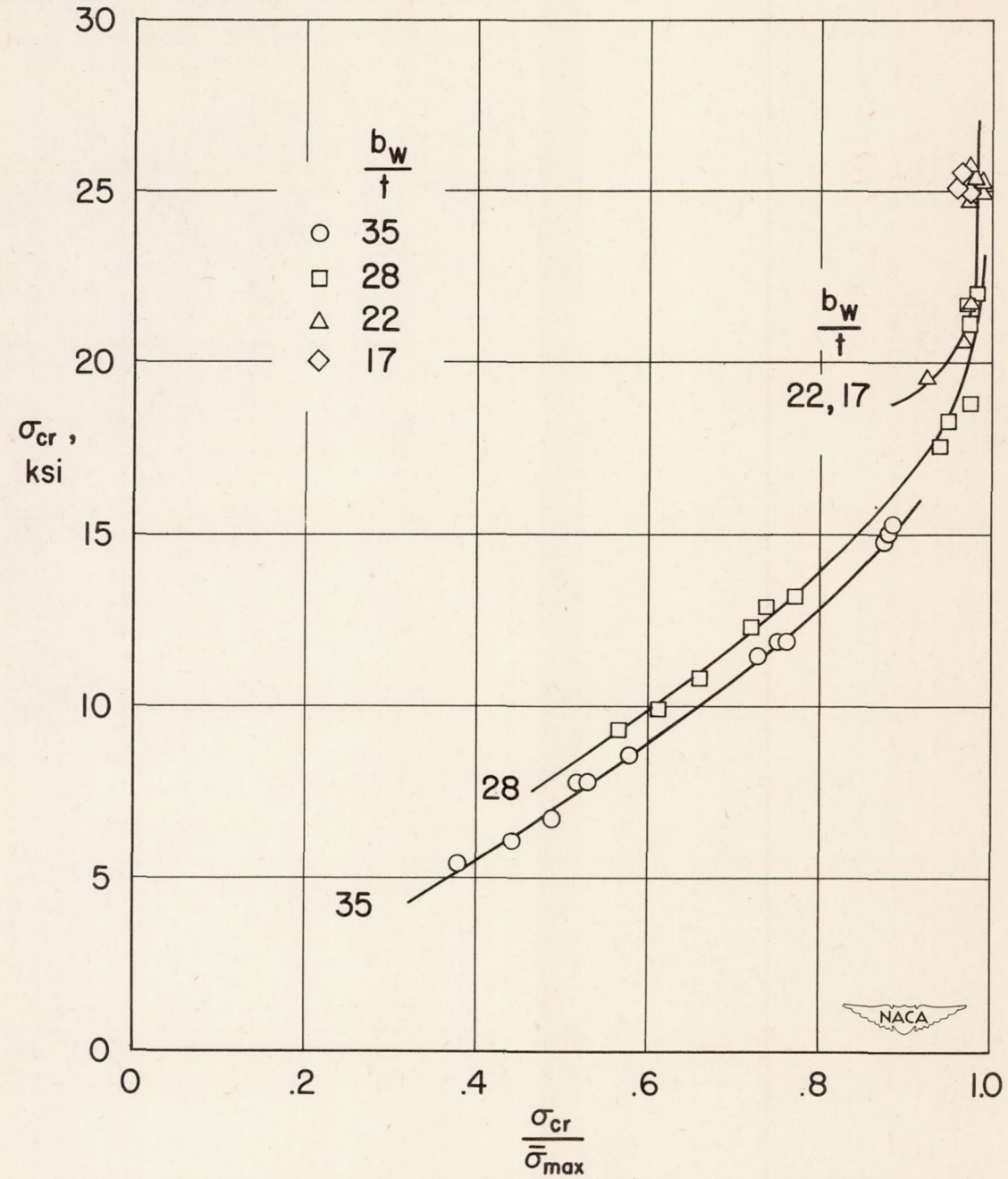

Figure 8.— Experimental relationship between σ_{cr} and $\bar{\sigma}_{max}$ for FS-Ih magnesium-alloy formed Z-section columns.

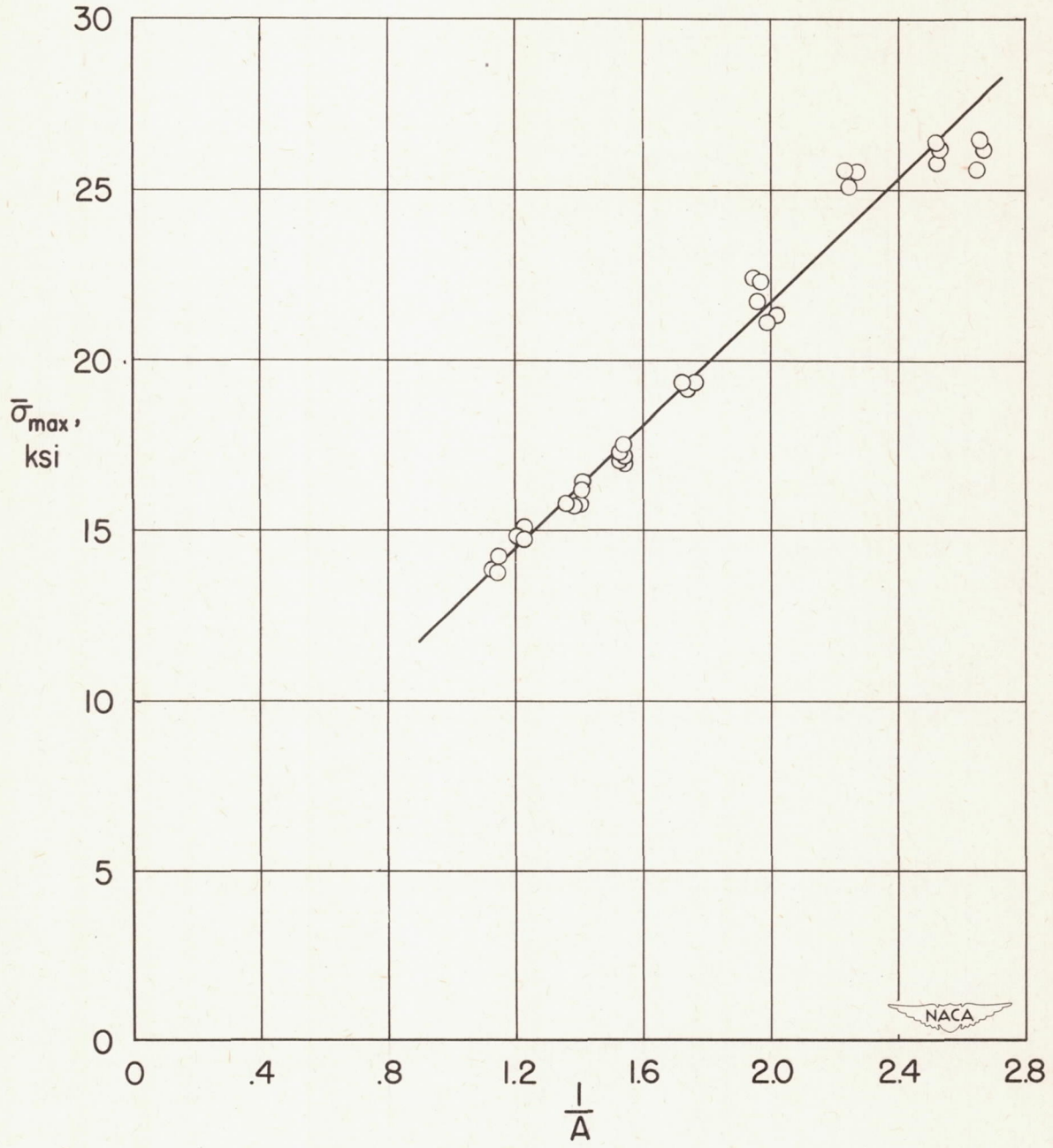

Figure 9.— Variation of $\bar{\sigma}_{max}$ with the reciprocal of the area for FS-1h magnesium-alloy formed Z-sections.

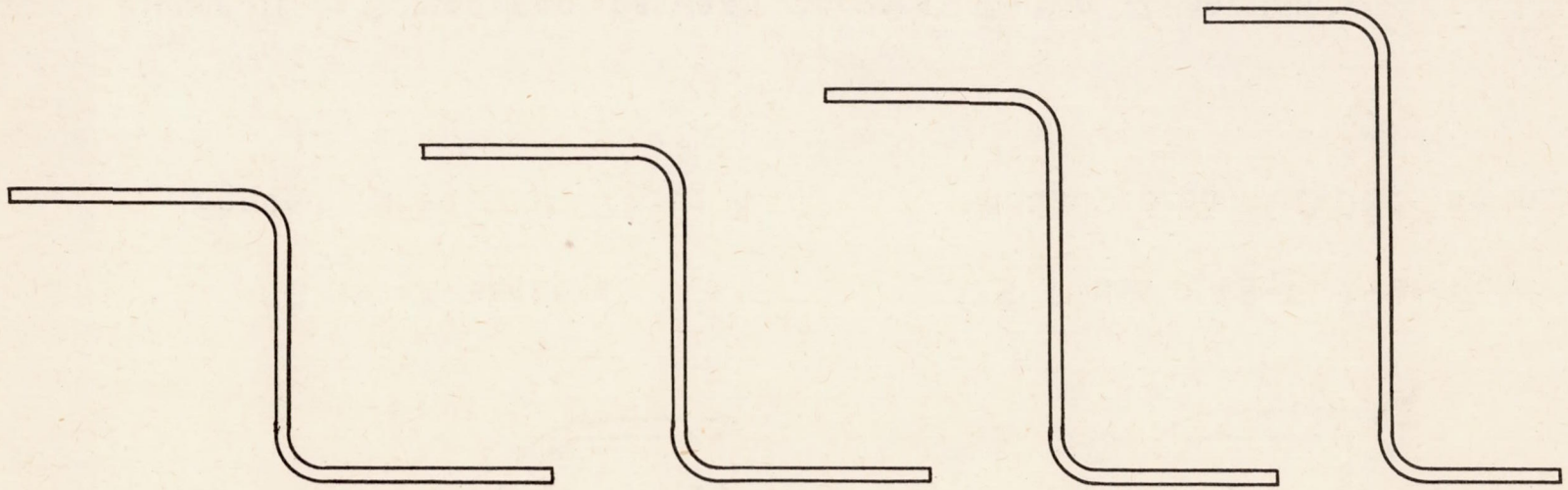

Column	13a	16a	21c	26c
Area, sq in.	1.039	1.045	1.071	1.060
$\bar{\sigma}_{max}$, ksi	29.3	29.2	29.7	28.9
σ_{cr}, ksi	14.7	17.6	21.7	23.9

Figure 10. — Comparison of $\bar{\sigma}_{max}$ and σ_{cr} for several 24S-T aluminum-alloy formed Z-sections (from reference 3) of nominally equal thickness and area.

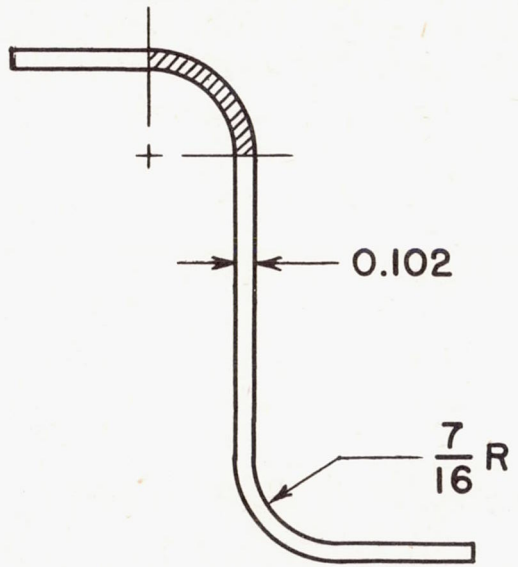

FS-1h Z-sections

Shaded area = 0.078 sq in.

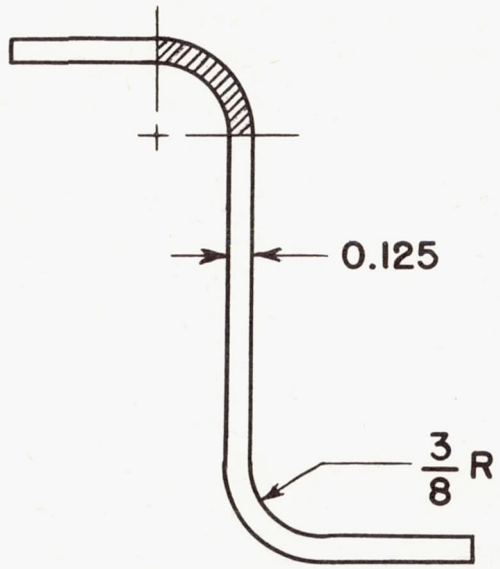

17S-T and 24S-T Z-sections

Shaded area = 0.086 sq in.

Figure 11.— Comparison between corners of two Z-sections.

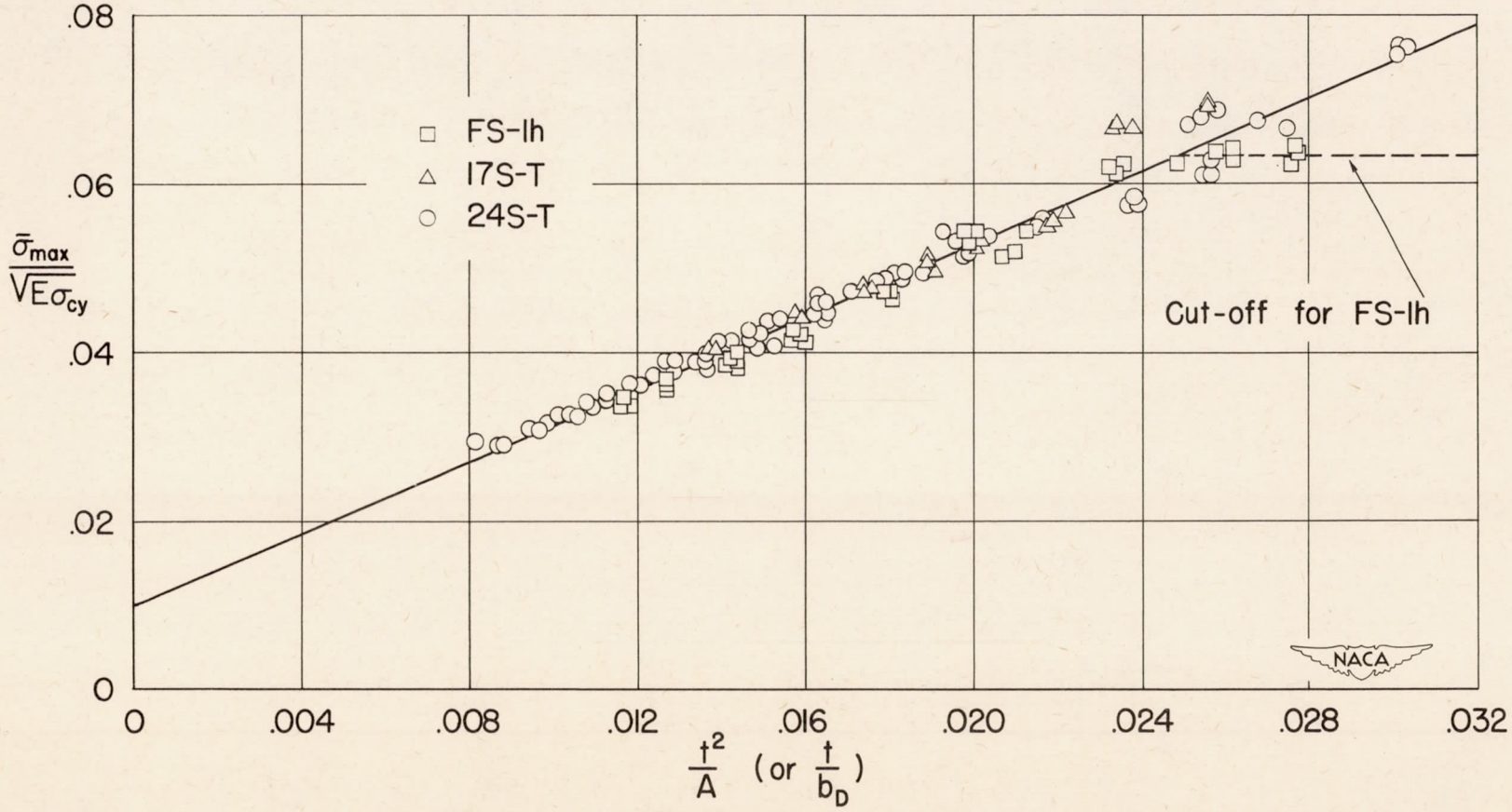

Figure 12.— Variation of $\bar{\sigma}_{max}/\sqrt{E\sigma_{cy}}$ with t^2/A for formed Z-sections of FS-Ih magnesium alloy and 17S-T and 24S-T aluminum alloys.